Phys. Rev. 102, 1501 (1956).
[36]M. B. Stearns and S. S. Wilson, Phys. Rev. Letters 13, 313 (1964).
[37]P. G. de Gennes, J. Phys. Radium 23, 630 (1962).
[38]A. J. Heeger, A. P. Klein, and P. Tu, Phys. Rev. Letters 17, 803 (1966).
[39]K. Handrich, Phys. Status Solidi 32, K55 (1969).
[40]C. G. Montgomery, J. I. Kruger, and R. M. Stubbs, Phys. Rev. Letters 25, 669 (1970).
[41]R. J. Elliot, B. R. Heap, D. J. Morgan, and G. S. Rushbrooke, Phys. Rev. Letters 5, 366 (1960).
[42]H. Sato, A. Arrott, and R. Kikuchi, J. Phys. Chem. Solids 10, 19 (1959).
[43]D. H. Martin, *Magnetism in Solids* (MIT Press, Cambridge, 1967).
[44]Pol Duwez (private communication).
[45]W. J. Schuele, S. Shtrikman, and D. Treves, J. Appl. Phys. 36, 1010 (1965).
[46]A. R. Kaufmann, S. T. Pan, and J. R. Clark, Rev. Mod. Phys. 17, 87 (1945).
[47]W. E. Henry, Phys. Rev. Letters 11, 468 (1963).
[48]P. P. Craig and W. A. Steyert, Phys. Rev. Letters 13, 802 (1969).
[49]U. Gonser, R. W. Grant, C. J. Meecham, A. H. Muir, Jr., and H. Wiedersich, J. Appl. Phys. 36, 2124 (1965).
[50]R. J. Borg, R. Booth, and C. E. Violet, Phys. Rev. Letters 11, 464 (1963).
[51]C. E. Violet and R. J. Borg, Phys. Rev. 149, 540 (1966).
[52]O. S. Lutes and J. L. Schmidt, Phys. Rev. 134, A676 (1964).
[53]E. Scheil, H. Specht, and E. Wachtel, Z. Metallk. 49, 590 (1958).
[54]S. T. Pan, A. R. Kaufman, and F. Bitter, J. Chem. Phys. 10, 318 (1942).
[55]A. N. Gerritsen, Physica 25, 489 (1959).
[56]M. Hansen, *Constitution of Binary Alloys* (McGraw-Hill, New York, 1966), p. 20.

PHYSICAL REVIEW B VOLUME 5, NUMBER 3 1 FEBRUARY 1972

Effect of Pressure on the Ferromagnetic Transition of $MnAs_xSb_{1-x}$ Solid Solutions*

L. R. Edwards and L. C. Bartel
Sandia Laboratories, Albuquerque, New Mexico 87115
(Received 28 July 1971)

The ferromagnetic transition temperatures of $MnAs_xSb_{1-x}$ solid solutions for $0 \leq x \leq 1$ have been measured as a function of pressure up to 4.5 kbar. Previous work has shown that for the solid solutions in the concentration range $0.9 \lesssim x \leq 1$ the magnetic transition is first order and is accompanied by a hexagonal-to-orthorhombic structure transformation, while for $0 \leq x \lesssim 0.9$ the magnetic transition is second order with no structural change. We have found that the initial pressure derivative of the transition temperature ($\partial T_c/\partial P$) changes discontinuously in the narrow concentration range $0.87 \lesssim x \leq 0.90$, further demarcating the first- and second-order regions. We also find that substituting Sb for As in the first-order region increases the critical pressure P_c which stabilizes the orthorhombic phase to the lowest temperature. This further supports Goodenough's observation of a critical molar-volume range in which the first-order transformation occurs. The solid solutions which exhibit second-order behavior are analyzed using an itinerant-electron ferromagnet model.

I. INTRODUCTION

The isomorphic metallic compounds MnAs and MnSb have different magnetic properties which are believed to be due to differences in the Mn-Mn separation distance. For increasing temperature, MnAs exhibits a first-order ferromagnetic (FM) to paramagnetic (PM) transition at 313 °K which is accompanied by a change in crystal symmetry from the hexagonal NiAs structure ($B8_1$) to the orthorhombic MnP structure ($B31$). (Hereinafter we use FM to denote ferromagnetic, ferromagnet, or ferromagnetism, and similarly for PM.) On further heating, a second-order transition involving a change from a low-spin PM to a high-spin PM phase and a change in crystal symmetry from the orthorhombic ($B31$) to hexagonal structure[1] ($B8_1$) is observed at 398 °K. On the other hand, MnSb has a second-order FM to PM transition at 572 °K with the crystal structure remaining hexagonal ($B8_1$) through the transition.[2] A complete series of solid solutions is formed by MnAs and MnSb in which the hexagonal lattice parameters decrease monotonically from MnSb to MnAs.[3]

The various magnetic transition temperatures and crystal structures of the solid solutions, $MnAs_xSb_{1-x}$ as reported by Sirota and Vasilev[4] and Goodenough *et al.*[5] are summarized in Fig. 1. Here, for increasing temperature, T_c denotes the FM-to-PM transition temperature, T' denotes the PM-to-PM transition temperature at which the effective moment decreases, and T_t is a PM-to-PM transition temperature at which the effective moment increases and the crystal structure changes

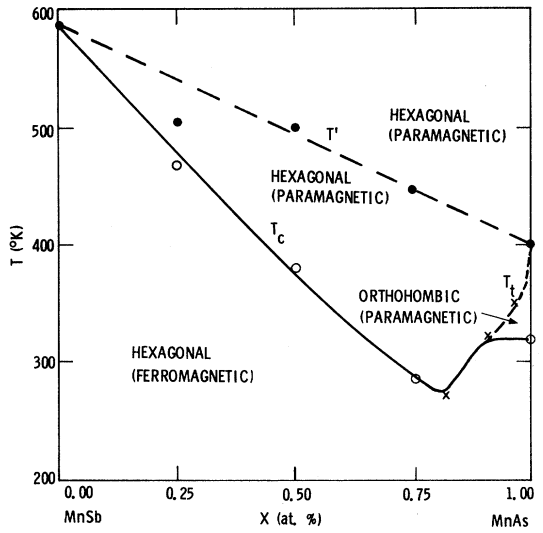

FIG. 1. Magnetic transition temperatures of $MnAs_xSb_{1-x}$ solid solutions. Open circle, solid circle after Sirota and Vasilev (Ref. 4) and × after Goodenough *et al.* (Ref. 5).

from orthorhombic to hexagonal. For the solid solutions in the concentration range $0.9 \leq x \leq 1.0$ the transition from the FM hexagonal phase to the PM orthorhombic phase is first-order. All other transitions are second order.

From Fig. 1 we see that over the concentration range $0 \leq x \leq 0.80$ the FM-to-PM transition temperature T_c decreases with increasing As concentration. In addition, the effect of substituting As for Sb is to decrease the lattice parameters[3] (decrease the Mn-Mn separation distance); thus one might expect T_c to be quite sensitive to pressure and to decrease with the application of pressure. As we shall report in Sec. II, we have observed a decrease in T_c with increasing pressure for solid solutions in this concentration range.

Goodenough and co-workers have proposed a band model to explain some of the magnetic properties of MnAs.[1,5,6] The essential features of their model are a filled s-p bonding (valence) band and an empty s-p antibonding (conduction) band where the Fermi energy lies between the bonding and antibonding bands, and the Mn $3d$ states lie near the Fermi energy. In the hexagonal FM phase the crystalline field splits the Mn $3d$ states into three distinct energy levels labeled t_0, $t_\pm$, and e_g.[6] The t_0 orbital is directed toward the nearest-neighbor (nn) Mn along the c axis, the two $t_\pm$ orbitals are directed toward nn Mn in the basal plane, and the two e_g orbitals are directed toward nn As. It is also argued that there is a critical Mn-Mn separation ($R_c \sim 3.1$–3.7 Å) such that an itinerant description is used if the Mn-Mn separation is less than R_c and a localized description is used if the Mn-Mn separation is greater than R_c.[1,7] Since the Mn-Mn separation is less than R_c along the c axis, the t_0 and e_g levels broaden into narrow itinerant bands.[8] However, in the basal plane the $t_\pm$ levels are transitional since the Mn-Mn separation can be greater or less than R_c depending upon the crystallographic phase. Finally in their model, it is postulated that there is an intra-atomic exchange splitting between the up- and down-spin bands.

Over the entire concentration range of the solid solutions, the Mn-Mn separation distance along the c axis remains less than R_c, and thus the t_0 and e_g levels should be narrow itinerant bands. One might then expect that an itinerant-electron model may describe the pressure dependence of the FM-to-PM transition. The weak itinerant-electron theory as developed by Wohlfarth[9] and Edwards and Wohlfarth[10] has been used to study the magnetic behavior of such materials as $ZrZn_2$[9] and the Invar alloys.[11] Recently, Wohlfarth and Bartel[12] have shown how to estimate electron-correlation effects from pressure measurements for weak itinerant FM's. In Sec. III, we extend the itinerant-electron model to include the so-called strong itinerant FM's and this model will be used to analyze the experimental data presented in Sec. II for only those solid solutions in the concentration range $x < 0.9$ where these materials exhibit a second-order behavior.

It has been established in MnAs that above a critical pressure of 4 kbars the orthorhombic phase is stabilized.[1,6] According to Goodenough and Kafalas,[6] the existence of this critical pressure is related to a critical molar volume. Within this critical molar volume there is a high- to low-spin transition which they interpret as a "drastic" change in the intra-atomic exchange energy at a maximum critical bandwidth. Then as we substitute Sb for As the lattice expands and the bandwidth decreases so that a higher critical pressure should result for stabilizing the orthorhombic phase. Since the orthorhombic phase exists in the solid solutions only over the concentration range $0.90 \leq x \leq 1$, we have measured the pertinent part of the pressure-temperature magnetic-phase diagram of the solid solution $MnAs_{0.90}Sb_{0.10}$. The maximum allowable Sb concentration was chosen to maximize the increase in critical pressure. These results will also be presented in Sec. II and discussed in Sec. III.

II. EXPERIMENTAL RESULTS

For the preparation of the solid solutions, powders of 99.9% pure Mn, As, and Sb were mixed to the desired proportions, pressed into pellets, sealed in an evacuated quartz tube, and heated to 1073 °K for 2 days. The chemically reacted product was then crushed, made into pellets, and annealed at 1073 °K for 1 day. There were no ob-

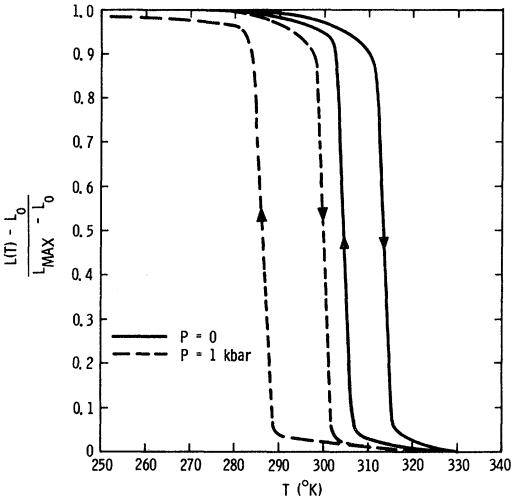

FIG. 2. A typical self-inductance–vs-temperature plot for the $x = 0.9$ solid solution. $L(T)$ is the temperature-dependent inductance, L_{max} is the maximum value of $L(T)$, and L_0 is the minimum value of $L(T)$.

served differences in the magnetic transitions or chemical composition if the samples were quenched in air or were slowly furnace cooled. Chemical analysis of these materials indicated they were stoichiometric to within 4 at. % and the ratio of As to Sb was within 1 at. % of the nominal value. Powder x-ray-diffraction patterns indicated the presence of MnO in some of the solid solutions. The presence of MnO should not affect the magnetic transition temperatures of these materials.

The self-inductance technique[13,14] was used to determined the FM-to-PM transition as a function of pressure and temperature. Hydrostatic pressure was applied with a 4.5-kbar helium-gas system[15] on the solid solutions which had transition temperatures less than 323 °K and with a Harwood 30-kbar liquid-pentane apparatus on the solid solutions which had transition temperatures greater than 323 °K. A typical reduced self-inductance–temperature plot as obtained for the $MnAs_{0.9}Sb_{0.1}$ solid solution is shown in Fig. 2. The transition temperature was arbitrarily taken as the half-transition point.

The experimental results are summarized in Figs. 3–5. In Fig. 3, the FM-to-PM transition temperature T_c is plotted as a function of concentration. The double curve in the concentration range $0.9 \leq x \leq 1.0$ is due to the thermal hysteresis associated with the first-order, hexagonal-FM-to-orthorhombic-PM, transition. No hysteresis is observed for the solid solutions in the concentration range $0 \leq x < 0.90$ which is indicative of a second-order FM-to-PM transition. Hereinafter we will refer to $0.9 \leq x \leq 1.0$ as the first-order region and to $0 \leq x < 0.9$ as the second-order region.

In Fig. 4, the initial pressure derivative of the FM-to-PM transition temperature ($\partial T_c / \partial P$) is plotted as a function of concentration. The pressure derivatives were determined to within ±0.15 °K/kbar. For MnSb, our measured pressure derivative of −3.0 °K/kbar is in good agreement with the value −3.2 °K/kbar as reported by Hirone *et al.*[16] It is observed that $\partial T_c / \partial P$ changes almost precipitously in a very narrow concentration range (~3%) demarcating the first- and second-order regions. It should be remarked that the $x = 0.88$ material exhibited no thermal hysteresis at 4.5 kbar—indicating that the transition remained second order up

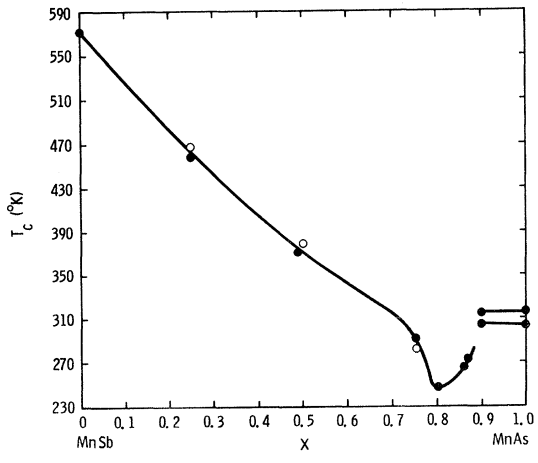

FIG. 3. Concentration dependence of the FM-to-PM transition temperature, in $MnAs_xSb_{1-x}$ solid solutions. Solid circle, present study; open circle, after Sirota and Vasilev (Ref. 4).

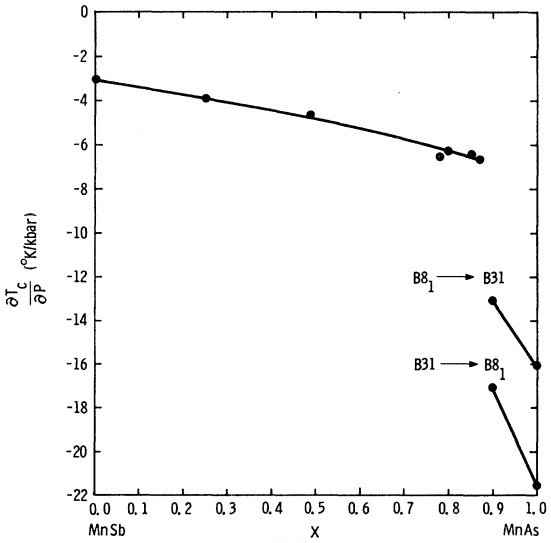

FIG. 4. Concentration dependence of the initial pressure derivative of the FM-to-PM transition temperature in $MnAs_xSb_{1-x}$ solid solutions.

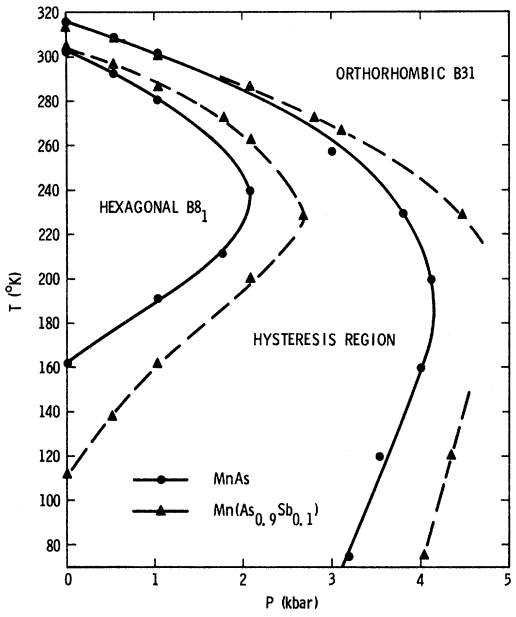

FIG. 5. Temperature-vs-pressure magnetic-phase diagram for MnAs and $MnAs_{0.9}Sb_{0.1}$.

to this pressure limit. (According to the Bean-Rodbell model, [17] it is possible that a second-order transition can be forced into a first-order transition under sufficient pressure; we shall comment more on this in Sec. III.

In Fig. 5, a portion of the temperature-pressure magnetic-phase diagram for MnAs and $MnAs_{0.9}Sb_{0.1}$ is shown. Our results for MnAs are in good agreement with the result of Menyuk *et al.* [1] It is observed, as speculated in Sec. I, that the substitution of 10% Sb for As does indeed increase the critical pressure required to stabilize the orthorhombic phase. The increase in critical pressure is approximately 0.75–1 kbar.

III. DISCUSSION

In Sec. III A, we discuss the solid solutions which exhibit second-order behavior. The results on these materials will be analyzed in terms of an itinerant-electron FM model. In Sec. III B, the alloys which exhibit a first-order behavior will be discussed in terms of the model proposed by Goodenough and Kafalas. [6] In addition, some comments will also be made on the Bean-Rodbell model[17] prediction of pressure-induced second-order to first-order behavior and on the equivalence of the itinerant-electron FM and the Bean-Rodbell models.

A. Second-Order Behavior

1. *Itinerant-Electron FM Model*

It is our purpose here to present an elementary theory, unifying several existing theories, of a single-band itinerant-electron FM. In particular, we shall develop a theory, appropriate for 3*d* electrons, for the Curie temperature T_c and its pressure derivative $\partial T_c/\partial P$; and we shall show how estimates of the effective exchange I times the density of states at Fermi level $N(\epsilon_F)$ can be made from the measurements of $\partial T_c/\partial P$. The theory presented here follows quite closely the earlier work of Wohlfarth, [9] Edwards and Wohlfarth, [10] Shiga, [18] and Wohlfarth and Bartel, [12] but includes details which have not been discussed in these earlier works.

For our model we assume that the exchange splitting is given by $nI\zeta$, where I is the effective intra-atomic exchange (accounting for the electron correlations) between the itinerant electrons, n is the number of d electrons per atom, and ζ is the relative magnetization per electron arising from single-particle excitations. In the Stoner theory, the exchange splitting is $2k_B\theta'\zeta$, where $k_B\theta'$ is the molecular-field-approximation interaction; thus $k_B\theta' = \frac{1}{2}nI$. The single-particle excitations are described by the Stoner equations, [9,10] and in the limit of $\zeta \to 0$ for $T \to T_c$ we have, using a Sommerfeld expansion, that T_c is given by[19]

$$T_c^2 = T_F^2(\overline{I} - 1)/\overline{I} \quad , \tag{1}$$

where

$$\overline{I} = IN(\epsilon_F) \, . \tag{2}$$

Here $N(\epsilon_F)$ is the density of states per atom per spin at the paramagnetic Fermi level, and T_F is the effective degeneracy temperature. [9,10] In order for the system to be FM, we have from Eq. (1) the Stoner criterion $\overline{I} \geq 1$. In the following discussion we shall make some assumptions as to the nature of I and $N(\epsilon_F)$.

In general, we assume that the effective intra-atomic exchange between the itinerant electrons I is a compositionally averaged constant in the case of the FM behavior of alloys. For the $MnAs_xSb_{1-x}$ solid solutions considered in this paper, I is the effective exchange appropriate for the Mn atoms. The particular form we shall use for I has been discussed by previous authors[12,18,20,21] and is given here as

$$I = I_b\,(1 + \gamma I_b/W)^{-1} \, , \tag{3}$$

where I_b is the bare interaction, W is the bandwidth, and γ is a constant. In addition, we assume that the number of magnetic electrons n remains constant, [22] consequently $N(\epsilon_F)$ can be written as[12,18]

$$N(\epsilon_F) = \beta/W \quad , \tag{4}$$

where β is another constant and is related to γ. It is implied that W and thus $N(\epsilon_F)$ scale uniformly (uniform-scaling assumption) under volume changes.

Finally, we assume the volume dependence of W is given by Heine's[23] results

$$\frac{\partial \ln W}{\partial \ln V} = -\frac{5}{3} \quad . \tag{5}$$

Using the above results, Eqs. (3)–(5), the volume dependence of $\bar{I}$, Eq. (2), is[12]

$$\frac{\partial \ln \bar{I}}{\partial \ln V} = \frac{5}{3}\,\frac{I}{I_b} \quad , \tag{6}$$

which is independent of β and γ and where here I_b is assumed independent of volume. For the density of states of the form given by Eq. (4), it can be shown that $T_F \sim W$, and hence from Eq. (5), $\partial \ln T_F / \partial \ln V = -\frac{5}{3}$. Using Eqs. (1), (2), (5), and (6) the volume dependence of T_c becomes

$$\frac{\partial \ln T_c}{\partial \ln V} \equiv \Gamma = -\tfrac{5}{3} + \tfrac{5}{6}\,(\bar{I}-1)^{-1}(I/I_b) \,. \tag{7}$$

In terms of pressure, Eq. (7) can be written as

$$\frac{\partial T_c}{\partial P} = \tfrac{5}{3}\kappa T_c - \tfrac{5}{6}\kappa\,\frac{I}{\bar{I} I_b}\,\frac{T_F^2}{T_c} \quad , \tag{8}$$

where κ is the volume compressibility and we have used Eq. (1).

We shall now show how pressure measurements of T_c can be used to determine a maximum value for $\bar{I}$ and a minimum value for T_F. The maximum value that I can have is the bare exchange value I_b; thus, the maximum value for the ratio I/I_b is one. Hence, the experimental value of Γ can be used to determine the maximum values of $\bar{I}$. From Eq. (7) we have

$$\bar{I}_{\max} = 1 + \tfrac{5}{6}\,(\Gamma + \tfrac{5}{3})^{-1} \quad . \tag{9}$$

Then using values for $\bar{I}$ obtained from Eq. (9) we can obtain a minimum value for T_F using Eq. (1).

For weak itinerant-electron FM's $\bar{I} \gtrsim 1.0$ and for weak electron-correlation effects $I/I_b \cong 1.0$, the second term in Eq. (7) is dominant, and from Eq. (8) we have $\partial T_c/\partial P \sim -1/T_c$. Examples of weak itinerant-electron FM's are the Fe-Ni, Fe-Pt, and Fe-Pd Invar alloys where it has been experimentally observed that $\partial T_c/\partial P \cong -\text{const}/T_c$.[24] For strong itinerant-electron FM's $\bar{I} > 1$ and for strong correlation effects $I/I_b < 1$ such that the first term in Eq. (7) is dominant, and from Eq. (8) we have $\partial T_c/\partial P \sim T_c$. An example of a strong itinerant-electron FM is Ni, where it is found that $\partial T_c/\partial P = \frac{5}{3}\kappa T_c \cong 0.68$ °K/kbar in good agreement with experimental values of 0.32–0.42 °K/kbar.[9] It is noteworthy that in the limit of weak itinerant-electron FM and for large Γ such that $|\Gamma| \gg \frac{5}{3}$ and neglecting the volume dependence of I_b, the results of this paper reduce to the results given previouly by Wohlfarth and Bartel.[12]

The localized and the itinerant, or collective, descriptions of magnetic electrons have been investigated by Goodenough.[25] He considered the case of one d electron per relevant d orbital which correponds to a half-filled band or to a half-filled localized orbital, and the magnetic order is antiferromagnetic (AFM). In the absence of competing exchange interactions, the Néel temperature T_N for localized-electron AFM increases with the transfer integral b since the exchange interaction is proportional to b^2; whereas, it has been shown that T_N for a band AFM decreases with increasing bandwidth[25,26] where the bandwidth is proportional to b. Goodenough concludes that the magnetic moment and T_N should vary continuously in going from a localized to a band description. We expect b to increase with increasing pressure; hence, we expect that for the localized electron description T_N should increase with increasing pressure, and for the itinerant description T_N should decrease with increasing pressure.[26] Furthermore, we expect that the general arguments for an AFM apply to the FM case of interest here. The observed decrease in the FM-to-PM transition temperature in the $MnAs_xSb_{1-x}$ compounds suggests that the itinerant-electron description is the appropriate one. Although these compounds are anisotropic, the isotropic model discussed in this paper describes the pressure effects quite well.

2. *Analysis of Experimental Results*

In Fig. 6, $\partial T_c/\partial P$ is plotted as a function of T_c for the $MnAs_xSb_{1-x}$ solid solutions in the concentration range $0 \leq x \leq 0.8$. For comparison, the Fe-Ni, Fe-Pd, and Fe-Pt Invar alloy data of Wayne and Bartel[24] are included. Similar to the Invar alloys, we observe a T_c^{-1} type of behavior as predicted by Eq. (8) when the second term in Eq. (8) dominates.

The volume derivative of T_c is calculated from $\partial T_c/\partial P$ where the compressibility for the solid solutions was obtained by a linear extrapolation between the values of $(2.5 \pm 0.5) \times 10^{-3}$ kbar^{-1} for MnSb[27] and 4.55×10^{-3} kbar^{-1} for MnAs.[1] The values for Γ are given in Table I. We observe that the values of Γ increase with increasing As concentration and that the magnitude of Γ is of the same order of magnitude as the first term in Eq. (7). In previous works on the Invar alloys[11,12] and $ZrZn_2$,[9–12] it was observed that $\Gamma \gg \frac{5}{3}$ and so the first term of Eq. (7) could be neglected. In the case of the $MnAs_xSb_{1-x}$ solid solutions, this factor of $\frac{5}{3}$ must be included in any calculation of band parameters.

In Table I, we give the results of the calculation of $\bar{I}_{\max}$ from Eq. (9) for the solid solutions $0 \leq x \leq 0.80$. The quoted error in the compressibility for MnSb will introduce an uncertainty of ± 0.03 in the value for $\bar{I}_{\max}$. We observe that $\bar{I}_{\max}$ decreases with increasing As concentration. According to Wohl-

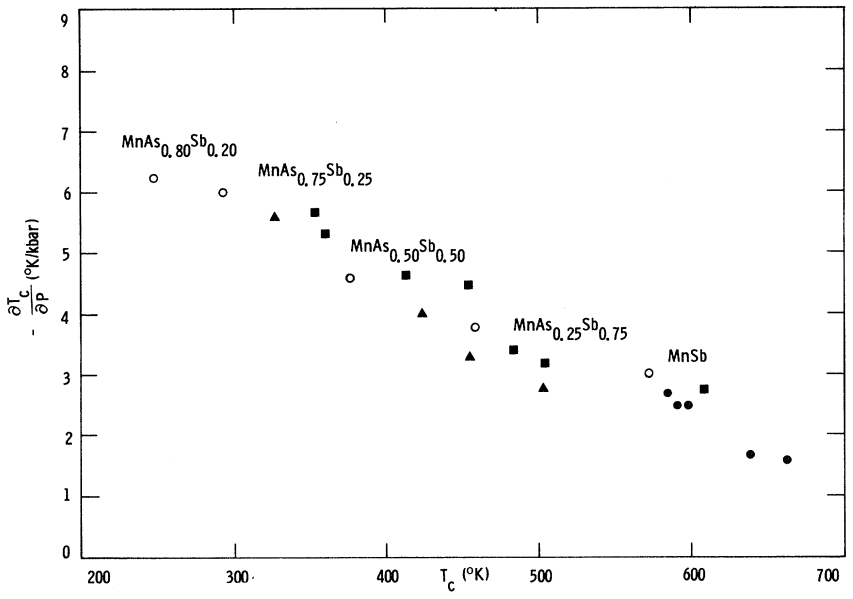

FIG. 6. A comparison of $\partial T_c/\partial P$-vs-T_c plots for various alloy systems. Open circle, $MnAs_xSb_{1-x}$; triangles Fe-Pt; solid circle, Fe-Pd; and square, Fe-Ni.

farth's[28] classification, these values of $\bar{I}_{max}$ indicate that MnSb is approaching a strong itinerant FM, and the solid solutions are becoming weaker itinerant FM's with increasing As concentration. These values of $\bar{I}_{max}$ for the $MnAs_xSb_{1-x}$ solid solutions are comparable with the values for the Invar alloys.[29]

From Eq. (1), and using the value of $\bar{I}$ and T_c for MnSb from Table I, we calculate $T_F = 1380\,^\circ\mathrm{K}$. Thus for MnSb we see that $T_c \cong 0.4T_F$ which indicates the Sommerfeld expansion is converging; however, the convergence is slower than one would desire. For the materials with $x > 0$, the convergence is more rapid than for $x = 0$.

Using Eqs. (1)–(4), we can express T_c as a function of the bandwidth W where we assume $T_F \sim W$. Then using the value of $T_c = 572\,^\circ\mathrm{K}$ and the value of $\bar{I}_{max}$ from Table I for MnSb, we can calculate T_c as a function of W. The results of these calculations are shown in Fig. 7. These results are independent of the value of I/I_b,[30] but do not include effects of any volume dependence of I_b. Note the critical bandwidth such that for $W/W_0 \geq 1.206$ we do not have FM order, and note the quadratic dependence of T_c on W for $W/W_0 \lesssim 1.206$. Using the available x-ray data[31] to estimate W/W_0 and using the experimental values for T_c we show, in Fig. 7, the experimental results of T_c as a function of W/W_0. For $x = 0.25$ we calculate $T_c = 474\,^\circ\mathrm{K}$ and $\bar{I} = 1.110$ in fair agreement with the experimental values. For the solid solutions $x > 0.25$ the agreement is only qualitative. This disagreement is not too surprising because of the large differences in unit-cell volumes for the various compositions. For these large volume differences one might expect significant changes in the crystal-field splittings, and consequently significant changes in the electronic wave functions. Any volume dependence of I_b would modify the results shown in Fig. 7. Lacking specific-heat, susceptibility, and magnetostriction data for these materials, we cannot determine $N(\epsilon_F)$, I, I_b, and any volume dependence of I_b individually. In addition, as we shall point out below, we expect rather large electron-lattice and exchange-striction interactions for these materials, particularly for the solid solutions $x \gtrsim 0.80$. Electron-lattice and exchange-striction effects have not been included in the calculations displayed in Fig. 7.

Sirota and Vasilev[4] have observed a Curie-Weiss type of behavior in the PM region for MnSb, with a Curie constant, $C_M = 1.3$ emu mole^{-1} Oe^{-1} °K^{-1}. According to the itinerant FM model of Wohlfarth[9] the susceptibility in the temperature region $T_F \gg T > T_c$ and for $T \to T_c$ can be written as $\chi \simeq \chi_0 T_c \times (T - T_c)^{-1}$ which is a Curie-Weiss type of behavior where the Curie constant C_M is given by $C_M = \chi_0 T_c$. The quantity χ_0 is proportional to $N(\epsilon_F)(\bar{I} - 1)^{-1}$.[9] For MnSb, χ_0 can be calculated to give $\chi_0 = 0.227$

TABLE I. Curie temperature T_c, $\Gamma \equiv \partial \ln T_c/\partial \ln V$, and $\bar{I}_{max}$, as calculated from Eq. (9), for various solid solutions of $MnAs_xSb_{1-x}$ in the second-order region.

x(at.% As)	T_c	Γ	$\bar{I}_{max}$
0.00	572	2.38	1.206
0.25	458	2.97	1.180
0.50	375	3.63	1.157
0.75	292	5.18	1.122
0.80	247	6.20	1.106

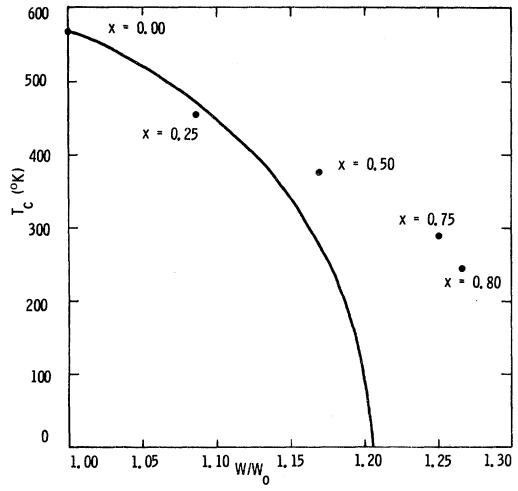

FIG. 7. A comparison of the calculated and experimental dependence of T_c on bandwidth, solid line, calculated; solid circle, experimental.

$\times 10^{-2}$ emu mole^{-1} Oe^{-1} as compared to $\chi_0 = 1.38 \times 10^{-2}$ emu mole^{-1} Oe^{-1} for $ZrZn_2$.[14] This difference in χ_0 between MnSb and $ZrZn_2$ is consistent with the values of $\bar{I}$ for these materials. For $ZrZn_2$,[9] $\bar{I} = 1.0042$ and from this work for MnSb, $\bar{I}_{max} = 1.206$; thus χ_0 for MnSb should be smaller. A detailed comparison,[32] however, can only be made if $N(\epsilon_F)$ for MnSb were known. For $x > 0$, χ_0 cannot be reliably extracted from the experimental data because the susceptibility has a complicated temperature dependence[4] which is thought to be due to exchange-striction effects.

B. First-Order Region

Previous experimental studies[6] on MnAs and $MnAs_xP_{1-x}$ have established that a first-order, hexagonal-FM-to-orthorhombic-PM, transition occurs only if the molar volume at T_c lies within a narrow critical range $V_t - \Delta V < V < V_t$, where $\Delta V/V \cong 0.025$. This narrow molar-volume range is related through the thermal expansion to the temperature range $T_t - 125\,^\circ\mathrm{K} < T < T_t$, where T_t is the second-order, orthorhombic-PM-to-hexagonal-PM, transition temperature. This, coupled with the fact that there is a low-spin $\rightleftharpoons$ high-spin transition in this temperature interval, led Goodenough and Kafalas[6] to postulate the existence of a maximum critical bandwidth that would support spontaneous FM and the existence of a volume-dependent intra-atomic exchange interaction. This model predicts the existence of a critical pressure P_c above which the PM orthorhombic phase is stabilized to absolute zero; a $P_c = 4$ kbar has been found for MnAs.[1,6] If P is substituted for As, than one expects P_c to decrease since the substitution of P decreases the lattice parameters (the molar volume), and thus the bandwidth increases. Furthermore, if sufficient P is substituted for As, $P_c \rightarrow 0$. These effects have been observed.[5,6] However, if Sb is substituted for As, the lattice parameters (molar volume) increase and the bandwidth decreases. Therefore, the substitution of Sb should cause P_c to increase, which is in accord with our experimental results.

Now if more than 10% Sb is substituted for As, then the molar volume will be larger than the critical volume required for a first-order transition, and the resulting solid solutions exhibit second-order transitions. If this model is correct, then at sufficiently high pressure one might expect to induce a first-order phase change in the materials with concentration $x \lesssim 0.9$. At the time this work was done, the pressures available to us (~ 4kbar) were insufficient to check conclusively this prediction on the $x = 0.88$ solid solution. Estimations based on the isotropic Bean-Rodbell model[17] indicate a second- to first-order transition pressure of approximatly 16 kbar for this material. This number must be taken lightly, however, since there have been objections to using the Bean-Rodbell model in its isotropic form for MnAs.[1] We are planning to continue the search for a second- to first-order transition pressure at higher pressure in the solid solutions with concentrations $x \lesssim 0.9$.

The Bean-Rodbell model,[17] which is based on a localized spin picture, has been used to describe qualitatively the first-order nature of the transition in MnAs. A similar situation arises in the itinerant electron model when the exchange and electron-lattice forces are balanced against the elastic forces. The result of this balance is that the bandwidth and exchange interaction become temperature dependent; then, depending on the parameters, the transition may tend to sharpen and may become first-order as in the Bean-Rodbell model. This type of procedure has been used to explain thermal expansion effects in an itinerant-electron AFM[26] where only the electron-lattice interaction was considered. In this case it was demonstrated that the balance set up between the elastic and electron-lattice forces is important in explaining the anomalous behavior of the thermal expansion for temperatures near T_N. However, for the parameters used in the theory, no first-order nature was observed in the phase transition.[26] It is anticipated that inclusion of exchange-striction effects could precipitate a first-order phase transition for the itinerant-electron AFM.

Unpublished x-ray data by Goodenough[33] on $MnAs_{0.80}Sb_{0.02}$ show that the unit-cell volume is quite temperature dependent for temperatures near T_c where the volume decreases continously from a value of 70.81 Å^3 at a temperature of approximately 100 °K below T_c to a value of approximately 70.19 Å^3 at T_c. This represents approximately 0.9% decrease

in the volume. For MnAs there is approximately a 1.8% discontinuous volume decrease at T_c for increasing temperature. It is therefore apparent that for $x \gtrsim 0.80$ there are large interactions of the lattice with the exchange energy and/or the electronic energy. The volume changes associated with these interactions depend on the magnetization. Because of the coupling, a discontinuous change in the unit-cell volume is reflected in a discontinuous change in the magnetization, and vice versa.

The physical picture we have for the results of the coupling of the magnetization and the lattice is as follows. At low temperature the magnetization takes on its saturation value, and the magnetic characteristics are determined by the bandwidth W, density of states $N(\epsilon_F)$, and the exchange interaction I. As the temperature is increased the lattice expands, and because of electron-lattice coupling and exchange striction, W decreases and I can either increase or decrease depending on the sign of $\partial \ln I/\partial \ln V$. For the material under consideration here, as W decreases, T_c will increase and the magnetization for $T \ll T_c$ will increase over the value it would have had if W and I did not depend on the volume. However, because of the electron-lattice and exchange-striction effects, the lattice contracts for $T \lesssim T_c$ and thus W increases and T_c decreases. Hence depending upon the amount of coupling, the rate at which W increases (or the apparent T_c decreases) determines whether the transition will be second or first order. For the first-order transition, in the words of Bean and Rodbell,[17] "... this situation is like that of a man who has run beyond the brink of a cliff; there is no gentle way down." The critical volume discussed by Goodenough and Kafalas[6] appears to be intimately related to the electron-lattice and exchange-striction effects as a detailed theory should show.

Finally, the rather large changes in T_c with pressure for the first-order region are noteworthy. As shown in Fig. 4, there is a discontinuous change in $\partial T_c/\partial P$ at the composition which demarcates the boundary between the first- and second-order regions. In addition, there are strong hysteresis effects in the first-order region. At this time, we can offer no concrete explanation of the rather large $(\partial T_c/\partial P)$'s for the first-order region except to say that the large pressure effects appear to be connected to a "critical volume"[6] and consequently to the electron-lattice and exchange-striction effects.

We conclude that for the first-order region electron-lattice and exchange-striction effects are important, and that inclusion of these effects in an itinerant-electron FM model (which is in a similar spirit to the Bean-Rodbell model) will be able to explain in some detail the magnetic and structural behavior. We also conclude that although the itinerant model used to discuss the second-order region is rather simple, it contains in it the essential features of a more elaborate treatment.

ACKNOWLEDGMENTS

The authors gratefully acknowledge Dr. G. A. Samara for useful discussions, Dr. J. B. Goodenough for his x-ray data on the $x = 0.80$ solid solution, and J. D. Pierce for expert technical assistance.

---

*Work supported by the U. S. Atomic Energy Commission.

[1]N. Menyuk, J. A. Kafalas, K. Dwight, and J. B. Goodenough, Phys. Rev. 177, 942 (1969).

[2]R. H. Wilson and J. S. Kasper, Acta Cryst. 17, 95 (1964).

[3]W. Köster and E. Braun, Ann. Phys. (Leipzig) 4, 66 (1959).

[4]N. N. Sirota and E. A. Vasilev, Phys. Status Solidi 28, K175 (1968).

[5]J. B. Goodenough, D. H. Ridgley, and W. A. Newman, in *Proceedings of the International Conference on Magnetism, Nottingham*, 1964 (The Institute of Physics and the Physical Society, London, 1965).

[6]J. B. Goodenough and J. A. Kafalas, Phys. Rev. 157, 389 (1967).

[7]J. B. Goodenough, *Magnetism and the Chemical Bond* (Wiley, New York, 1963).

[8]There must be 3*d* itinerant-electron states to account for the metalliclike electrical conductivity as observed in MnAs and MnSb [G. Fischer and W. B. Pearson, Can. J. Phys. 36, 1010 (1958)] and in $(Cr_xMn_{1-x})Sb$ [T. Suzuoka, J. Phy. Soc. Japan 12, 1344 (1957)].

[9]E. P. Wohlfarth, J. Appl. Phys. 39, 1061 (1968); J. Phys. C 2, 68 (1969).

[10]D. M. Edwards and E. P. Wohlfarth, Proc. Roy. Soc. (London) A303, 127 (1968).

[11]J. Mathon and E. P. Wohlfarth, Phys. Status Solidi 30, K131 (1968); E. P. Wohlfarth, Phys. Letters 28A, 569 (1969); 31A, 525 (1970).

[12]E. P. Wohlfarth and L. C. Bartel, Phys. Letters 34A, 303 (1971).

[13]G. A. Samara and A. A. Giardini, Rev. Sci. Instr. 36, 108 (1965).

[14]R. C. Wayne and L. R. Edwards, Phys. Rev. 188, 1042 (1969).

[15]J. E. Schirber, Cryogenics 10, 418 (1970).

[16]T. Hirone, T. Kaneko, and K. Kondo, in *Physics of Solids at High Pressure*, edited by C. T. Tomizuka and R. M. Emrich (Academic, New York, 1965), p. 298.

[17]C. P. Bean and D. S. Rodbell, Phys. Rev. 126, 104 (1962).

[18]M. Shiga, Solid State Commun. 7, 559 (1969).

[19]The factor $\bar{I}$ in the denominator of Eq. (1) does not appear in the previous work.

[20]N. D. Lang and H. Ehrenreich, Phys. Rev. 168, 605 (1968).

[21]J. Kanamori, Progr. Theoret. Phys. (Kyoto) 30, 275 (1963).

[22]If *s*-*d* overlap is a strong function of interatomic distance

this assumption is not valid. However, in this case the number of Mn atoms remains constant throughout the concentration range, and therefore we expect the number of magnetic d electrons to remain more or less constant.

[23]V. Heine, Phys. Rev. 153, 673 (1967).

[24]R. C. Wayne and L. C. Bartel, Phys. Letters 28A, 196 (1968).

[25]J. B. Goodenough, J. Appl. Phys. 39, 403 (1968).

[26]L. C. Bartel, J. Appl. Phys. 41, 5132 (1970).

[27]R. W. Lynch, J. Chem. Phys. 47, 5180 (1967).

[28]E. P. Wohlfarth (unpublished).

[29]L. C. Bartel and E. P. Wohlfarth, Bull. Am. Phys. Soc. 16, 351 (1971).

[30]If we assume a ratio I/I_b for MnSb, then I/I_b is fixed, through Eq. (3), for the solid solutions when $x>0$. The results shown in Fig. 7 are independent of the assumed value of I/I_b for MnSb.

[31]The lattice parameters for MnSb and MnAs at $T=20$ °C were taken from the work of B. T. M. Willis and H. P. Rooksby, Proc. Phys. Soc. (London) 67B, 290 (1954). To obtain values for the intermediate solid solutions a linear extrapolation was used as the data of Ref. 3 suggest.

[32]For $ZrZn_2$, the Fermi level lies at the peak in the density of states that has a full width of approximately 0.16 eV [G. S. Knapp, F. Y. Fradin, and H. V. Culbert, J. Appl. Phys. 42, 1341 (1971)].

[33]J. B. Goodenough (private communication).

PHYSICAL REVIEW B VOLUME 5, NUMBER 3 1 FEBRUARY 1972

Critical Region in Ferroelectric Triglycine Sulfate

K. Deguchi and E. Nakamura
Department of Physics, Faculty of Science, Hokkaido University, Sapporo, Japan
(Received 1 September 1971)

Careful measurements have been made for triglycine sulfate (TGS), in the vicinity of the critical point T_c, on the temperature dependence of the spontaneous polarization and the field dependence of the polarization at T_c. It is found that deviations from the mean-field theory occur only within $T_c - T < \Delta T_c \approx 5\times10^{-3}$ °C and $E < E_c \approx 0.5$ V/cm. The coherence length ξ_0 at 0 °K is calculated on the basis of Menyhárd's theory, which gives a condition for the breakdown of the mean-field theory. The minimum values of ξ_0 obtained by ΔT_c and E_c are 7 and 6 Å, respectively, which are very close to the average distance, 6.8 Å, between statistical units of TGS.

The behavior of ferroelectric crystals near the critical temperature is of much interest, because it is typical of the cooperative phenomena in which the long-range electrostatic interaction plays an important role. Recent studies on triglycine sulfate (TGS) have shown that the experimental results are well explained by the Weiss-type mean-field theory (classical theory) in the range of $|T - T_c| \gtrsim 3\times10^{-2}$ °C and $E \gtrsim 30$ V/cm, where E is an applied electric field.[1,2] Furthermore, Blinc suggested that inside these regions the value of critical exponents obtained by hysteresis measurements were very close to those predicted by the three-dimensional Ising model.[2] The careful measurement of the dielectric constant[3] shows, however, that the critical exponent has the classical value even at $T - T_c = 10^{-2}$ °C and -5×10^{-3} °C. The aim of this note is to report the results of careful measurements of the dielectric hysteresis and to examine the range of validity of the mean-field theory in the vicinity of the critical point.

The samples used in the present measurements were gold evaporated on both b surfaces. The 50-Hz hysteresis loops were displayed on the oscilloscope screen through a Sawyer-Tower circuit with phase compensation. The values of spontaneous polarization P_s were determined by photographs enlarged about four times. The experimental setup was almost the same as that previously reported.[3] Measurements were made in the cooling process

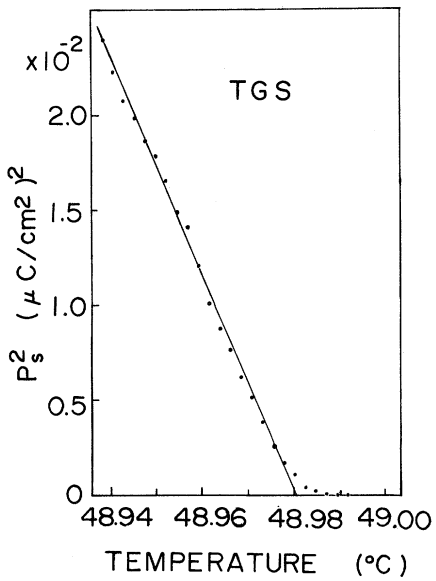

FIG. 1. Square of the spontaneous polarization vs temperature in TGS in the very vicinity of the Curie point.